

AD-A250 239**INATION PAGE**Form Approved
OMB No. 0704-0188

1

Public
maintains
suggest
and tofour per response, including the time for reviewing instructions, searching existing data sources, gathering and
tion. Send comments regarding this burden estimate or any other aspect of this collection of information, including
site for Information Operations and Reports, 1215 Jefferson Davis Highway, Suite 1204, Arlington, VA 22202-4302,
0188), Washington, DC 20503.

1. AGENCY USE ONLY (Leave blank)

2. REPORT DATE

March 1992

3. REPORT TYPE AND DATES COVERED

Professional paper

4. TITLE AND SUBTITLE

EVAPORATION DUCT EFFECTS AT MILLIMETER WAVELENGTHS

5. FUNDING NUMBERS

PR: SXBS
PE:
WU: DN888715

6. AUTHOR(S)

K. D. Anderson

7. PERFORMING ORGANIZATION NAME(S) AND ADDRESS(ES)

Naval Command, Control and Ocean Surveillance Center (NCCOSC),
Research, Development, Test and Evaluation Division (NRaD)
San Diego, CA 92152-50008. PERFORMING ORGANIZATION
REPORT NUMBER

9. SPONSORING/MONITORING AGENCY NAME(S) AND ADDRESS(ES)

Naval Command, Control and Ocean Surveillance Center (NCCOSC),
Research, Development, Test and Evaluation Division (NRaD)
San Diego, CA 92152-500010. SPONSORING/MONITORING
AGENCY REPORT NUMBER

11. SUPPLEMENTARY NOTES

DTIC
ELECTE
S MAY 18 1992 D
C

12a. DISTRIBUTION/AVAILABILITY STATEMENT

Approved for public release; distribution is unlimited.

12b. DISTRIBUTION CODE

13. ABSTRACT (Maximum 200 words)

The evaporation duct strongly influences low-altitude over-the-horizon propagation at millimeter wavelengths. Results from more than 2000 hours of propagation and meteorological measurements made at 94 GHz on a 40.6 km over-horizon, over-water path along the southern California coast show that that average received power was 63 dB greater than expected for propagation in a nonconducting, or standard, atmosphere; 90 percent of the measurements were at least 55 dB greater than diffraction.

A numerical model of transmission loss based on the observed surface meteorology is discussed and results are compared to measured transmission loss. On average, modeling results underestimate observations by only 10 dB. In addition, results from modelling based on an independent climatology of evaporation duct heights for the area are shown to be adequate for most propagation assessment purposes. The reliability and reasonable accuracy of the numerical model provides a strong justification for utilizing the technique to assess millimeter wave communication and radar systems operating in many, if not all, ocean regions.

Published in *AGARD Conference Proceedings No. 454*, October, 1989.

14. SUBJECT TERMS

electromagnetic propagation
electro-optics atmosphere

15. NUMBER OF PAGES

16. PRICE CODE

17. SECURITY CLASSIFICATION
OF REPORT

UNCLASSIFIED

18. SECURITY CLASSIFICATION
OF THIS PAGE

UNCLASSIFIED

19. SECURITY CLASSIFICATION
OF ABSTRACT

UNCLASSIFIED

20. LIMITATION OF ABSTRACT

SAME AS REPORT

UNCLASSIFIED

21a. NAME OF RESPONSIBLE INDIVIDUAL K, D. Anderson	21b. TELEPHONE (Include Area Code) (619) 553-1420	21c. OFFICE SYMBOL Code 543

AGARD

ADVISORY GROUP FOR AEROSPACE RESEARCH & DEVELOPMENT

7 RUE ANCIENNE 92200 NEUILLY SUR SEINE FRANCE

AGARD Paper Reprinted from
Conference Proceedings No.454

ATMOSPHERIC PROPAGATION IN THE UV,
VISIBLE, IR AND MM-WAVE REGION
AND RELATED SYSTEMS ASPECTS

*Copenhagen, Denmark, 9th-13th October 1989
paper 9, pps 9-1, 9-13*

NORTH ATLANTIC TREATY ORGANIZATION



92.5 13 064

92-12805



EVAPORATION DUCT EFFECTS AT MILLIMETER WAVELENGTHS

by

K.D. Anderson

Ocean and Atmospheric Sciences Division
 Naval Ocean Systems Center
 San Diego, CA 92152-5000
 United States



Summary

The evaporation duct strongly influences low-altitude over-the horizon propagation at millimeter wavelengths. Results from more than 2000 hours of propagation and meteorological measurements made at 94 GHz on a 40.6 km over-horizon, over-water path along the southern California coast show that the average received power was 63 dB greater than expected for propagation in a nonducting, or normal, atmosphere; 90 percent of the measurements were at least 55 dB greater than the normal atmosphere.

A numerical model of transmission loss based on observed surface meteorology is discussed and results are compared to measured transmission loss. On average, modeling results underestimate the transmission loss by 10 dB. In addition, results from modeling based on an independent climatology of evaporation duct heights for the area are shown to be adequate for most propagation assessment purposes. The reliability and reasonable accuracy of the model provide a strong justification for utilizing the technique to assess millimeter wave communication and radar systems operating in many, if not all, ocean regions.

LIST OF SYMBOLS

- δ Evaporation duct height (m).
 Δn Potential refractivity difference between air and sea.
 R Bulk Richardson's number.
 Γ Empirical profile coefficient.

INTRODUCTION

The evaporation duct is a nearly permanent propagation mechanism created by a rapid decrease of moisture immediately above the ocean surface. Air adjacent to the surface is saturated with water vapor and rapidly dries out with increasing height until an ambient value of water vapor content is reached, which is dependent on general meteorological conditions. The nearly logarithmic decrease in vapor pressure causes the refractivity gradient to decrease faster than -157 N/km, which is a trapping condition. The height at which dN/dz equals -157 N/km is defined as the evaporation duct height and is a measure of the strength of the duct. Typical duct heights are between a few meters and approximately 30 meters with a world-average value of 13.6 meters [1]. Because these ducts are vertically thin, strong trapping is infrequently observed for frequencies below 2 GHz.

For low-altitude, over-water applications, the evaporation duct has been shown to be a reliable propagation phenomena that can dramatically increase beyond-the-horizon signal levels for frequencies greater than 2 GHz [2]-[4]. Although the highest frequency reported in previous work is 35 GHz, the results show that the magnitude of signal enhancement (referenced to diffraction) increases with increasing frequency. An analysis of the Aegean Sea measurements [4] shows that median received signal power on a 35-km path is 2, 15, 27, and 30 dB above diffraction for frequencies of 1, 3, 9.6, and 18 GHz respectively. Received signal power at 35 GHz on this path is consistently 30 to 45 dB above diffraction [4].

Effects of evaporation ducting on over-the-horizon signal propagation at 94 GHz are presented. Results from more than 2000 hours of RF measurements made on a 40.6 km path along the southern California coast are analyzed in terms of path loss (equivalent to transmission loss) which is defined as the ratio of transmitted to received power assuming loss-free isotropic antennas. Numerical propagation modeling results based on measured and climatological surface meteorology are compared to measured path loss. These comparisons are good and the results strongly support using the propagation model to predict the performance of millimeter wave systems operating near the surface in all ocean regions.

A brief review of the evaporation duct model and the propagation model used in this analysis precedes a discussion of the experiment and the results.

Models

In practice, boundary-layer theory relates bulk surface meteorological measurements of air temperature, sea temperature, wind speed, and humidity to the vertical profile of refractivity and thus the evaporation duct height. In a thermally neutral atmosphere where the air-sea temperature difference is 0, the modified refractivity profile is given by

$$M(z) = M(0) + 0.125(z - \delta) \ln((z + z_0)/z_0) \quad (1)$$

where z is height above the ocean, δ is evaporation duct height, and z_0 is a length characterizing boundary roughness. For a thermally non-neutral atmosphere, stability terms are incorporated into Eq. (1) (See Jenks, [3]). However, for common departures from neutrality, propagation

Section For
 ORL
 TAB
 Woodward
 Classification

By _____	
Distribution/	
Availability On	
Dist	Avail and/c Special
A-1	

calculations indicate that a neutral profile is a reasonable approximation, provided that duct height for the neutral profile is calculated from observed meteorology. In this analysis, evaporation duct height is computed from surface observations using the Jeake model [3],[5] as implemented by Hitney [6] with thermal stability modifications suggested by Paulus [7].

Numerical propagation modeling techniques have shown good agreement to RF measurement results when single-station surface meteorological observations are available to determine the refractivity-versus-altitude profile of the evaporation duct [8]. In a maritime environment, the assumption of lateral homogeneity (vertical profile of refractivity invariant along the path of propagation) is generally good [8],[9] and justifies a waveguide formalism [10]-[12] approach to the analysis of propagation through the troposphere. Numerical results are derived from a computer program called "MLAYER" which is an enhanced version of the "XWVO" program [13]. MLAYER assumes that the vertical profile of refractivity over the sea can be approximated by an arbitrary number of linear segments and uses an ingenious technique [14] to find all complex modes that propagate with attenuation rates below a specified value. Surface roughness is developed from Kirchhoff-Huygens theory in terms of rms bump height, σ , which is related to wind speed as $\sigma = 0.0051u^2$, where u is wind speed (m/s) [15],[16].

The determination of the vertical refractivity profile is crucial to the MLAYER calculations. For neutral and stable conditions, the duct height is

$$\delta = \frac{-\Delta\phi_0}{1.32 + 0.0867 \cdot R/\Gamma \cdot (0.75 - \Delta\phi_0)} \quad (2)$$

where ϕ_0 is the potential refractivity difference between the air and sea surface, R is the bulk Richardson's number, and Γ is an empirical profile coefficient. Eq. (2) assumes that bulk parameters are measured at a height of 6 m and that z_0 is 0.00015 m. Under neutral conditions, R is zero, hence the potential refractivity difference is $\phi_0 = -1.32 \cdot \delta$. The potential refractivity gradient (under neutral and stable conditions) is

$$\frac{\Delta\phi}{\Delta z} = \frac{\Delta\phi_0 [1/z + 0.0867 \cdot R/\Gamma]}{10.60 + 0.52 \cdot R/\Gamma} \quad (3)$$

where z is the height above the surface. Again, under strictly neutral conditions, Eq. (3) reduces to $\Delta\phi/\Delta z = \Delta\phi_0/(10.60 \cdot z)$. The potential refractivity gradient is related to the refractivity gradient as

$\Delta\phi/\Delta z = \Delta N/\Delta z + 0.032$ and to the modified refractivity gradient as $\Delta\phi/\Delta z = \Delta M/\Delta z - 0.125$. Using Eqs. (2) and (3), the modified refractivity profile was determined for evaporation duct heights from 0 to 20 m in 2 m intervals. These profiles are shown in Fig. 1 where the surface modified refractivity is referenced to 0 M-units. Path loss calculations were made for five rms bump heights; 0.0 (smooth surface), 0.025, 0.100, 0.250, and 0.500 m corresponding to wind speeds of 0.0, 4.3, 8.6, 13.6, and 19.2 knots.

For a one-way transmission system, signal power at the receiver is

$$P_r = P_t + G_t - L + G_r + G_a \quad (4)$$

where P_t is power transmitted, G_t and G_r are transmitter and receiver antenna gains, and G_a is additional gain measured from the receiver antenna to the point in the receiver where power is measured. Assuming transmission-line losses and other hardware-related losses are accounted for in P_t or G_t , the loss L can be written as $L = L_m + L_e$, where L_m is loss due to molecular absorption and L_e is loss accounting for all other environmental and geometrical losses. The advantage of treating L as the sum of two independent terms is that L_m then depends on observable air temperature and humidity, whereas L_e depends on the same two observables in addition to sea temperature and wind speed. Of course, both loss terms depend on geometry of the transmission path; L_m is the product of attenuation rate and path length, and L_e involves a complicated dependency on the refractivity profile, path length, and antenna heights.

Range dependency of absorption-free path loss (L_e) at a frequency of 94 GHz is shown in Fig. 2 for a normal atmosphere, denoted by 0 duct height, and for evaporation duct profiles (neutral stability) corresponding to duct heights of 2, 4, 6, and 8 m. In this case, transmitter and receiver are 5 and 9.7 m above a smooth sea surface, and coherent signal propagation (modal phasing included) is assumed. At a range separation of 40 km, L_e for transmission through a normal atmosphere is about 250 dB (assuming a typical 0.7 dB/km molecular absorption attenuation rate, total path loss is about 280 dB). For propagation in an atmosphere represented by a refractivity profile corresponding to an evaporation duct height of two meters (a relatively shallow duct), L_e is approximately 184 dB -- a "gain" of 66 dB compared to the diffraction reference. With an 8-m evaporation duct, path loss increases with range at a fairly consistent rate of about 0.2 dB/km beyond 30 km.

Path loss variation with receiver height is shown in Fig. 3 for a path separation of 40.6 km. The transmitter is located 5 m above a smooth surface. In a normal atmosphere, path loss for a receiver located 20 m above the surface is about 230 dB. For this same receiver in an environment of a 2-m evaporation duct, path loss is about 178 dB; a gain of 52 dB even though both transmitter and receiver are outside of the duct.

Surface roughness effects are shown in Fig. 4 for a transmitter at 5 m, receiver at 9.7 m, and a fixed path separation of 40.6 km. Incoherent signal propagation (modal phase is ignored) is used to represent absorption-free loss, L_e . Higher wind speeds generally increase loss with respect to a smooth surface, except for a normal atmosphere where the waveguide modes are

evanescent. For duct heights above 10 m, path loss at the two highest wind speeds are nearly equal. Above 10 m, path loss for wind speeds greater than about 8 knots are nearly equal. In these highly trapped cases, many weakly attenuated modes are found and the aggregate effect is for convergence of the mode sums to a limiting value. At 94 GHz, the limiting value of surface roughness appears to be a bump height of 0.5 m.

EQUIPMENT DESCRIPTION

A 40.6-km transmission path along the Southern California coast was chosen and instrumented for the measurement program. The path is shown in Fig. 5. The transmitter antenna was located 5 m above mean low water (mlw) at the Dal Mar Boat Basin facility of the U.S. Marine Corps Base at Camp Pendleton, CA. This antenna, a horizontally polarized 12-inch-diameter lens with a 0.7° beamwidth, was centered along the path at an elevation angle of zero degrees. The horizon is 9.2 km and is shown as a dashed arc in Fig. 5.

The receiver site was at the western end of Scripps Pier, located at the University of California at San Diego, CA. This pier extended 335 m from the shore, which, in all but the worst storms, placed the receiver beyond the surf zone (this pier has since been torn down and replaced by a new structure). The receiver antenna was located 9.7 m above mlw (horizon of 12.9 km) and was pointed towards the transmitter with an elevation angle of zero degrees.

The RF transmitter was similar to the receiver which is shown in Fig. 6. An X-Band oscillator, phase-locked to a stable 103-MHz crystal source, phase-locked a 94-GHz Gunn diode. Approximately 23 dBm of transmitter power was generated by an injection-locked IMPATT diode. At the receiver, the 103-MHz crystal source was offset from the transmitter crystal reference to generate an IF of 59.8 MHz which was monitored by a spectrum analyzer. Although the controller could adjust analyzer functions to optimize signal detection, the analyzer was typically set for a frequency span of 181.7 KHz, no integration, and with video and resolution bandwidths of 3 KHz. Signal power and frequency were recorded with an effective sample time of 540 milliseconds.

System "constants" (power transmitted, antenna gains, and RF-to-IF gain of the receiver) are listed in Table 1. Total path loss is related to observed received signal power as $L = 157 - P_r$, which is the sum of the system constant minus the power received (see Eq. 4). Minimum detectable signal power at the analyzer was ≈ -83 dBm, which corresponds to a maximum detectable path loss of ≈ 240 dB ($L = 157 - -83$). Diffraction is about 250 dB for the geometry of the path (See Fig. 2). Therefore, without evaporation ducting, the signal should be 10 dB below the receiver noise level and should not be detectable. However, the expected gain of about 60 dB through evaporation ducting, less the expected molecular absorption loss of about 30 dB, places the signal at about 220 dB which is detectable by the receiver.

The dynamic range of the analyzer was sufficient to lock onto and track the signal in all conditions, except when there was precipitation along the path, which was rare. A moderate rain shower, uniform along the path, could increase path loss by 100 dB, making any practical reception impossible. As a reference, the basic free-space transmission loss, $(4\pi d/\lambda)^2$, is 164 dB, where d is the range separation and λ is the wavelength.

Air temperature, sea temperature, relative humidity, wind speed, and wind direction were recorded at Scripps Pier in conjunction with the RF measurements. Table 2 describes the surface meteorological sensors, which were monitored by a data acquisition system that sampled and stored the data every 10 seconds.

In operation, measurements were recorded 24 hours per day. To reduce the volume of data, statistics of rms and standard deviation were locally computed for 10-minute intervals. Approximately 60 samples of surface meteorology and approximately 1000 samples of power monitored at the analyzer were used to compute those statistics. The local data (statistics) were automatically transferred for further analysis via modem lines to computers at Naval Ocean Systems Center, about 10 miles south of the receiver site.

Evaporation duct height and molecular absorption were computed from observed rms values of surface meteorology. Absorption-free path loss was determined by a look-up procedure into a precomputed two dimensional table. One dimension of this table was evaporation duct height from 0 to 20 m in 2-m intervals; the other dimension was rms bump height specified at 0 (smooth surface), 0.25, and 0.50 m.

RESULTS

MEASUREMENTS

Measurements began in late July 1986 and continued through early July 1987. Eight periods, totaling 102 days of operations, were completed during this time. Table 3 lists the time periods in which measurements were made.

One-way transmission path data were analyzed by comparing observed rms path loss (transmission loss) to path loss computed for both evaporation duct height and rms bump height, which were calculated from surface meteorological quantities measured at the receiver site. Absorption-free path loss calculated by M-LAYER was modified by adding molecular absorption loss calculated from surface meteorology (reference [17]) in order to compare it to observed total path loss. Molecular absorption loss during the entire measurement program averaged approximately 30 dB.

Figure 7 shows the time-series of surface meteorology, measured path loss, and predicted path loss for a representative measurement period. Figure 7(a) is a time-series plot of measured air temperature (°C), relative humidity (%), and wind speed (knots). Also included in this figure is

the computed molecular absorption (dB), labeled as α . The time shown on the abscissa is plotted in local time; hour 00 is associated with the tic mark above the first character in the day label. Gaps in the data (around August 8) were due to software and hardware failures that were manually corrected.

In this period, relative humidity was nearly always greater than 90 % and accompanied with light winds. Sea temperature was fairly constant at about 20 degrees Celsius. Figure 7(b) shows the air-sea temperature difference and the calculated evaporation duct height. Diurnal changes of about 3 degree Celsius in air temperature are observed early in this period and become less pronounced later. Wind direction, Fig. 7(c), shows some land-sea breeze effects up until about August 4th when the breeze became fairly constant from the northwest. Fig. 7(d) shows the observed and predicted path loss. Predicted path loss is derived from $d_0^2 \times$ the calculated absorption to the path loss calculated for the evaporation duct height on a point-by-point basis. Considering that the propagation model assumes spatial and temporal homogeneity along the entire 40.6 km path, the time-series agreement between the observed and predicted path loss is remarkable.

With no evaporation ducting, the estimated path loss is the sum of the diffraction path loss and the molecular absorption. The diffraction loss for the path geometry is 230 dB; the average molecular absorption loss is seen to be about 35 dB (Fig. 7(a)); therefore the estimated path loss with no evaporation ducting is about 285 dB. From Fig. 7(d), the average observed path loss is about 225 dB, which is 60 dB less than what is expected using normal or 4/3 earth propagation prediction models. However, the observed path loss is about 60 dB greater than the free-space level (164 dB) which means that radar applications are unlikely unless the target has a large radar cross-section.

ALL MEASUREMENT PERIODS COMBINED

The crucial parameter that relates path loss to surface meteorological conditions is evaporation duct height. A scatter plot of difference between observed and predicted path loss in relation to calculated duct height is shown in Fig. 8. All 102 days of observations, more than 12,000 data points, are included. Predicted path loss, on average, underestimates observed path loss by approximately 10 dB and, in the extremes, underestimates by nearly 40 dB and overestimates by 22 dB. A trend line, computed from a histogram of scatter, indicates median error. The trend is for error to increase with duct height up to heights of about 5 m; median error is relatively flat for higher duct heights.

Wind speed strongly affects both evaporation duct height and surface roughness. Higher winds generally increase duct height and increase attenuation due to roughness. A scatter plot of error in path loss with relation to wind speed is shown in Fig. 9. A trend line indicates that median error is about 2.5 dB for winds less than 1 knot and increases to -14 dB at about 5 knots. For winds greater than about 5 knots, error remains nearly constant at about 14 dB. It is tempting to reduce the error bias by modifying rms bump height because the surface roughness formulation in M-LAYER is one of the largest uncertainties at millimeter wavelengths. However, the measurement program was designed to test for gross environmental effects; a modification to rms bump height or surface roughness formulation cannot be justified from this data.

CLIMATOLOGY

A comparison of observed absorption-free path loss to predictions derived from a separate climatology of evaporation duct heights [1] illustrates an application of the propagation model to the assessment of a millimeter wave system. The evaporation duct climatology is based on 15 years of surface meteorological observations (normally taken on ships at sea) from which the distribution of evaporation duct heights were computed. All ocean areas were analyzed in $10^\circ \times 10^\circ$ grids (Naradan Squares). For the San Diego off-shore area, the evaporation duct height frequency distribution, Fig. 18, shows a peak for duct heights between 6 and 10 m. Duct heights greater than 20 m are infrequent. Combining this distribution with the results shown in Fig. 4 (0.25 m bump height), gives an accumulated frequency distribution which is shown as a solid line in Fig. 11. Observed absorption-free path loss is plotted on the same figure as a dotted line. Free space and diffraction fields are referenced. Although the predicted path loss distribution consistently underestimates the observed, it is clearly a better predictor compared to assuming a normal atmosphere representation of the environment. In the worst case, it is only some 10 dB less than observed, whereas the difference is about 4 dB at the 50 percent level. The observed path loss reduction from diffraction exceeds 63 dB half of the time, 90 percent of the time the reduction exceeds 55 dB. Both predicted and observed distributions show that path loss is 45 dB less than the diffraction reference 100 percent of the time (the occurrence of rain was negligible during the measurements).

CONCLUSIONS

Low altitude propagation of millimeter waves at ranges beyond the radio horizon is strongly influenced by the evaporation duct; for the propagation path used, received power levels are on the order of 50 to 100 dB greater than the power levels expected for propagation through a nonducting or normal atmosphere.

A single-station measurement of surface meteorology is adequate to analyze millimeter wave propagation over the ocean. On a point-by-point comparison, modeling typically underestimates observations by about 10 dB; the error is probably due to incomplete considerations of both horizontal heterogeneity and surface roughness effects. Direct sensing of the environment on the scale of kilometers in the horizontal and meters in the vertical is impractical, however, planetary boundary layer models and remote sensing techniques may, in the future, offer

considerable improvement to the propagation analysis. The formulation of surface roughness in the propagation model is one area that is actively being examined for a more complete understanding.

In summary, the increase in received signal strength due to the presence of the evaporation duct has been realistically modeled and provides an accurate estimate of actual millimeter wave system performance. The significant system "gain" due to evaporation ducting is clearly an important consideration in the design stages of moderate range, over-water millimeter wave systems.

REFERENCES

- [1] W.L. Paterson, "Climatology of marine atmospheric refractive effects," Naval Ocean Syst. Gen. Tech. Doc. 573, 523 pp., December 1986.
- [2] M. Katzin, R.W. Bauchman, and W. Binnian, "3- and 9-centimeter propagation in low ocean ducts," Proc. IRE, vol. 35, pp. 891-905, September 1947.
- [3] H. Jeske, "Die Ausbreitung elektromagnetischer Wellen im cm- bis m-Band über dem Meer unter besonderer Berücksichtigung der meteorologischen Bedingungen in der maritimen Grenzschicht," Hamburger Geophys. Einzelschriften, Hamburg, DeGruyter and Co., 1965.
- [4] J.H. Richter and H.V. Hitney, "Antenna heights for the optimum utilization of the oceanic evaporation duct," Naval Ocean Syst. Gen. Tech. Doc. 1209, 313 pp., January 1988.
- [5] H. Jeske, "State and limits of prediction methods of radar wave propagation conditions over sea," paper presented at the NATO Advanced Study Institute, Sorrento, Italy, 5-16 June 1973.
- [6] H.V. Hitney, "Propagation modeling in the evaporation duct," Naval Electronics Lab. Gen. Tech. Rep. 1947, 38 pp., April 1975.
- [7] R.A. Paulus, "Practical application of an evaporation duct model," Radio Sci., vol. 20, pp. 887-896, 1985.
- [8] H.V. Hitney, J.H. Richter, R.A. Pappert, K.D. Anderson, and G.B. Baumgartner, Jr., "Tropospheric radio propagation assessment," Proc. IEEE, vol. 73, pp. 265-283, 1985.
- [9] H. Jeske, "The state of radar-range prediction over sea," Tropospheric Radio Wave Propagation Part II, AGARD, pp. 50-1,50-6, February 1971.
- [10] H.G. Booker and W. Walkinshaw, "The mode theory of tropospheric refraction and its relation to waveguides and diffraction," in Meteorological Factors in Radio Wave Propagation, London, England: The Physical Society, 1946, pp. 80-127.
- [11] K.G. Budden, The Waveguide Mode Theory of Wave Propagation. London, England: Logos Press, 1961.
- [12] L.M. Brekhovskikh, Waves in Layered Media, 2nd ed. New York: Pergamon, 1970.
- [13] G.B. Baumgartner, Jr., "XWVG: A waveguide program for trilinear tropospheric ducts," Naval Ocean Syst. Gen. Tech. Doc 610, 206 pp., June 1983.
- [14] D.G. Morfitt and G.R. Shellman, "MODESRGH", an improved computer program for obtaining ELF/VLF/LF mode constants in an earth atmosphere waveguide," Interim Rep 7-T, prepared for the Defense Nuclear Agency by the Naval Electronics Lab. Gen. (now Naval Ocean Syst. Gen.), 327 pp., October 1976.
- [15] W.D. Ament, "Toward a theory of reflection by a rough surface," Proc. IRE, vol. 41, pp. 142-146, 1953.
- [16] O.M. Phillips, Dynamics of the Upper Ocean. London: Cambridge Univ. Press, 1966.
- [17] H.J. Liebe, K.C. Allen, G.R. Hand, R.H. Espeland, and E.J. Violante, "Millimeter-wave propagation in moist air: modal versus path data," NTIA Report 85-171, 54 pp., March 1985.

Table 1 RF System Constants

Component	Value
Transmitter power	23 dBm
Transmitter antenna gain	47 dBi
Receiver antenna gain	47 dBi
Receiver RF-to-IF gain	40 dB

Table 2 Surface Meteorological Sensors

Sensor	Type	Accuracy	Response
Air temperature	Platinum RTD	0.1 deg c	10 sec
Sea temperature	Platinum RTD	0.1 deg C	30 sec
Relative humidity	Crystallite fiber	6 %	60 sec
Wind speed	Cup	1 %	1.5 m
Wind direction	Vane	1 deg	1.1 m

Table 3 Dates of Measurements

Start	End
July 29, 1986	August 10
September 2, 1986	September 11
October 7, 1986	October 20
November 18, 1986	November 23
December 1, 1986	December 23
January 13, 1987	January 30
May 4, 1987	May 14
June 30, 1987	July 5

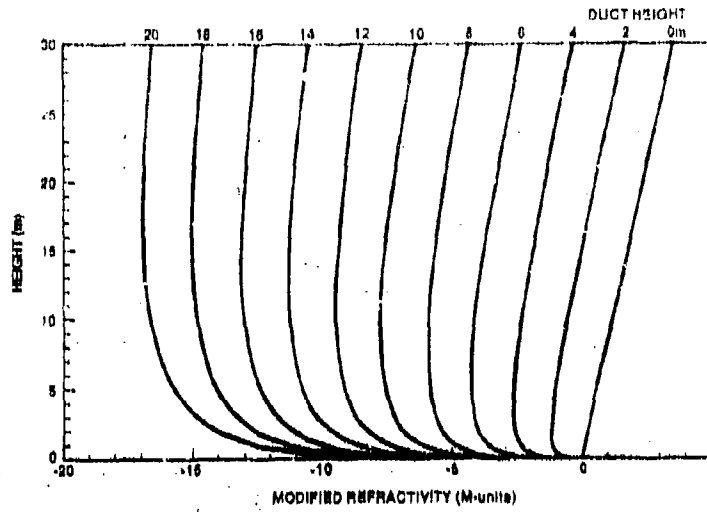


Fig. 1. Evaporation duct profiles for duct heights from 0 (normal) to 20 m in 2 m increments. Surface modified refractivity is referenced to 0 M-units.

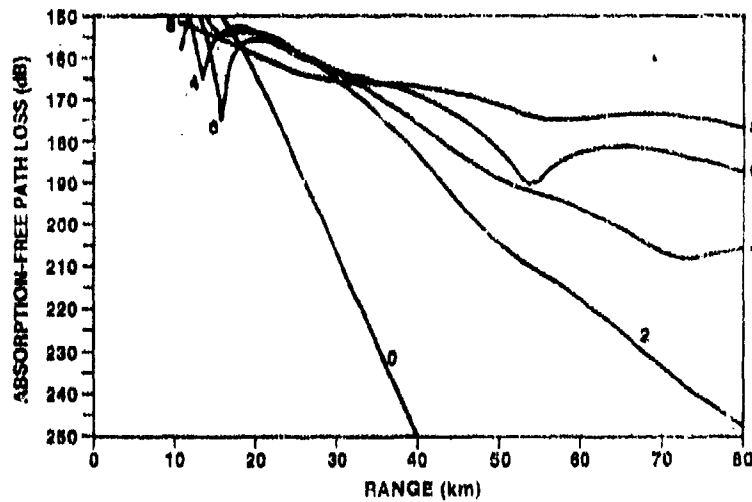


Fig. 2. Absorption-free path loss vs range for evaporation duct heights of 0 (normal), 2, 4, 6, and 8 m. Coherent mode summation and smooth surface.

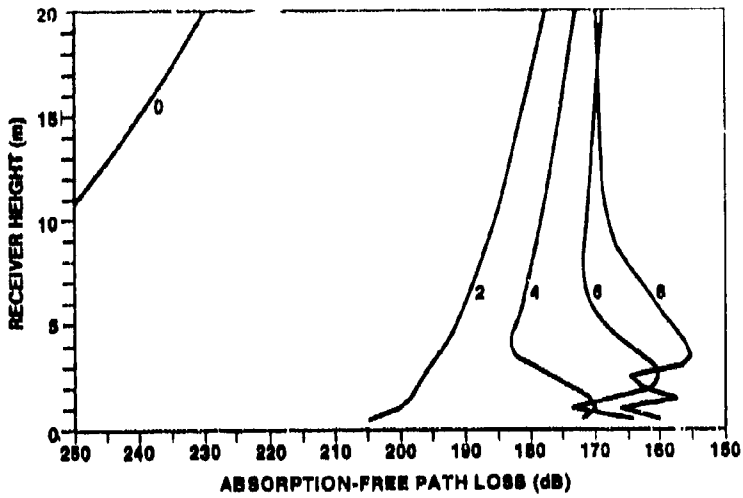


Fig. 3. Absorption-free path loss (incoherent) for a transmitter at 5 m, range separation of 40.6 km, and a smooth surface. The curves are labeled with the duct height.

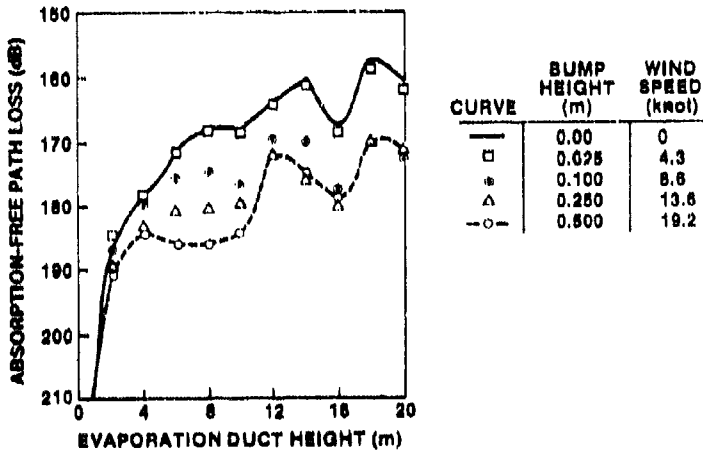


Fig. 4. Effects of surface roughness at 94 GHz. Transmitter at 5 m, receiver at 9.7 m, and range separation of 40.6 km. The rms bump height, expressing the surface roughness, is derived from Kirchoff-Huygens Theory (see Ament, 1953; Phillips, 1966).

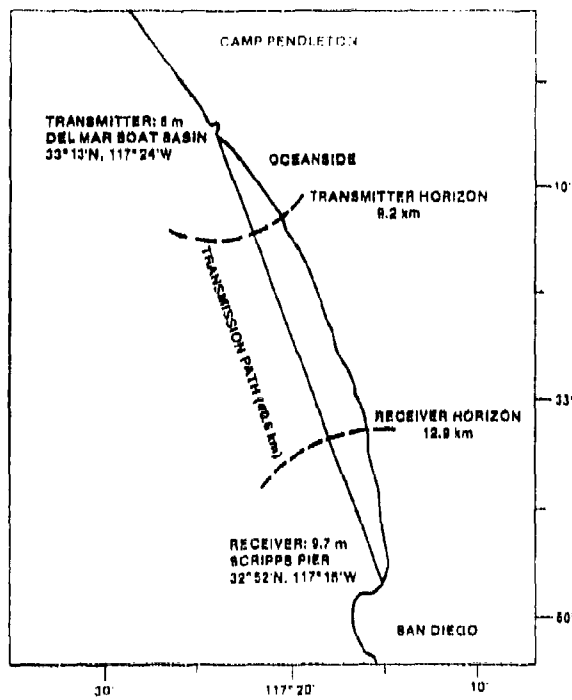


Fig. 5. Transmission path from Camp Pendleton to Scripps Pier, CA. Normal radio horizon is indicated by the dashed arcs centered on the transmitter and receiver sites.

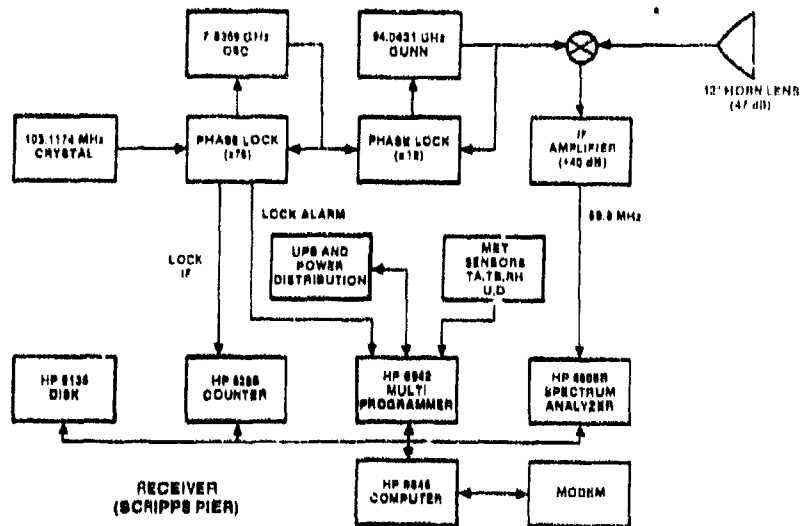


Fig. 6. Receiver system installed at Scripps Pier, CA.

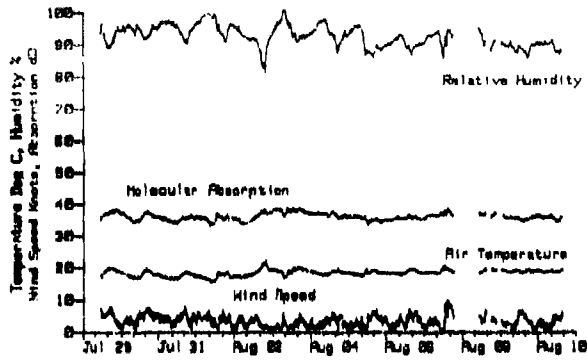


Fig. 7a. Air temperature, relative humidity, and wind speed measured at Scripps Pier. Molecular absorption at 94 GHz calculated from surface meteorological measurements.

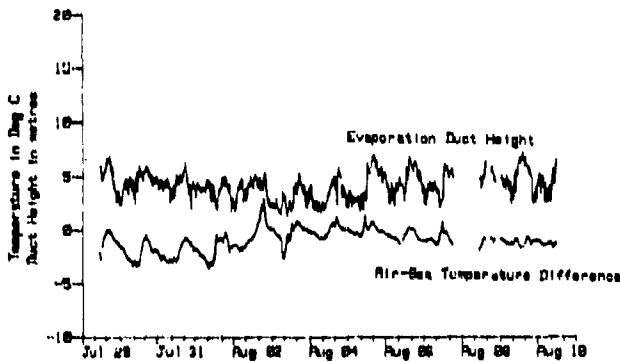


Fig. 7b. Air-sea temperature difference at Scripps Pier and calculated evaporation duct height.

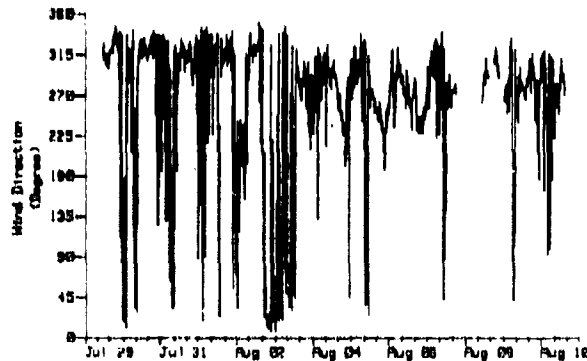


Fig. 7c. Wind direction at Scripps Pier.

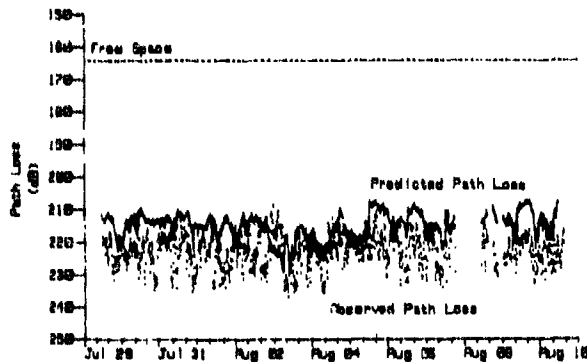


Fig. 7d. Measured path loss (dotted) and predicted path loss (solid).

Millimeter Wave Propagation Experiment
Jul 29 to Aug 10, 1986

Fig. 7. Meteorological and radio data recorded in the measurement period from July 29 to August 10, 1986. Predicted path loss, shown as the solid curve in Fig. 7d, tends to underestimate the measured path loss (dotted curve) by 10 dB.

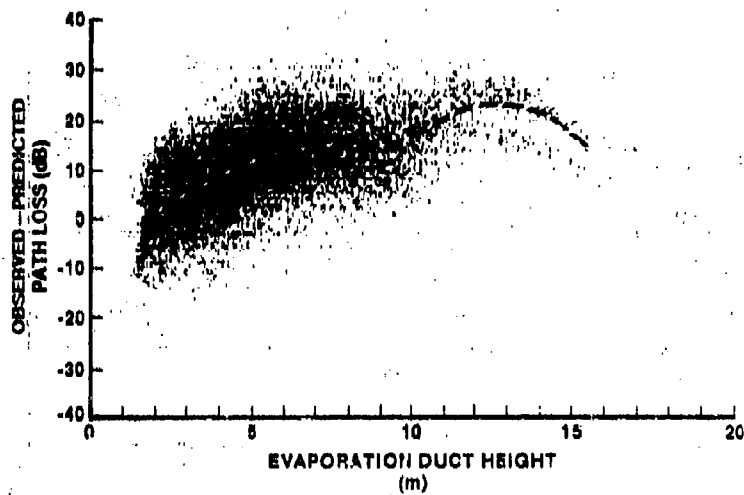


Fig. 8. Error (dB) between predicted and observed path loss in relation to observed evaporation duct height. All data measured, without qualification, are presented. A positive error indicates prediction underestimates observation

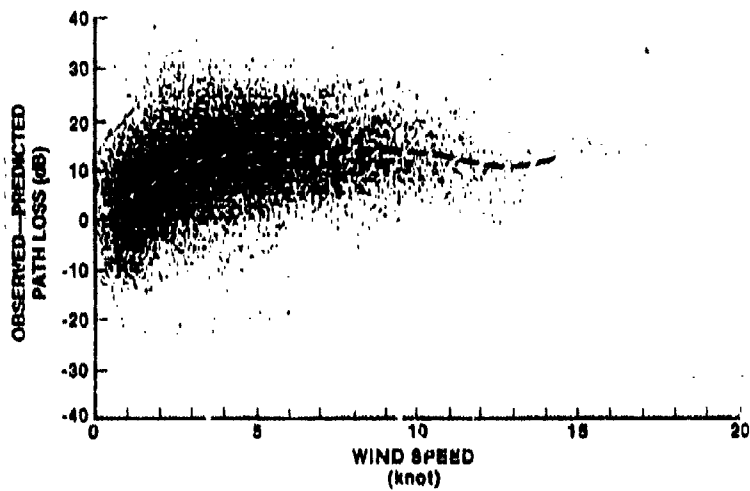


Fig. 9. Path loss error (dB) in terms of observed wind speed (knt) for all measurements.

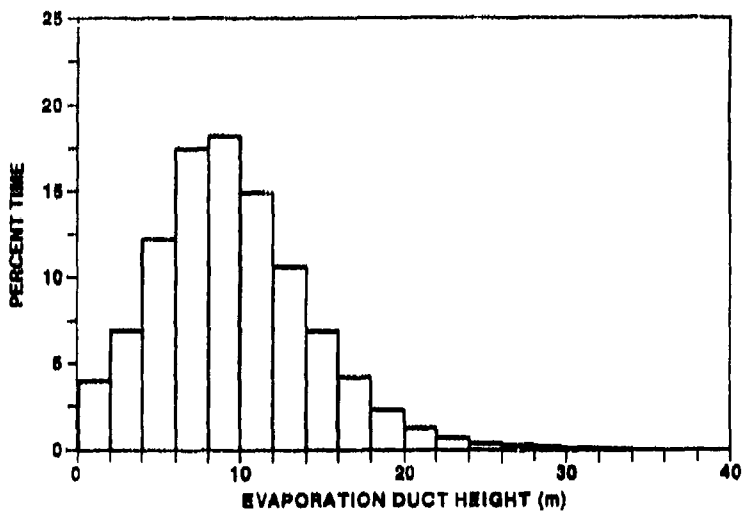


Fig. 10. Climatological evaporation duct height distribution for the San Diego off-shore area.

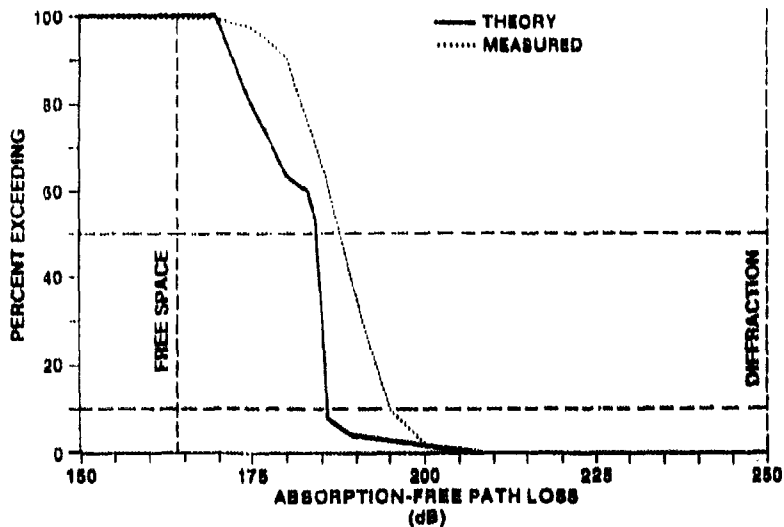


Fig. 11. Absorption-free path loss distribution predicted from the distribution in Fig. 10 compared to the measured (dotted curve). Total path loss can be approximated by reading the desired percentage and adding 30 dB (average absorption loss) to the corresponding abscissa coordinate.

DISCUSSION

M. LEVY

Does diffuse reflection from the rough sea surface contribute to transmission loss? Is it modeled? It might explain the discrepancy between measurements and prediction.

AUTHOR'S REPLY

We presently model sea surface roughness effects by simple modification of the reflection coefficient. A rigorous approach is being incorporated into our treatment using the parabolic equation approximation.

J. BACH ANDERSEN

Do you assume horizontal homogeneity of the duct, and could deviations explain the observed path loss?

AUTHOR'S REPLY

Yes, horizontal homogeneity is assumed and this is clearly not always correct. Spatial and temporal variations over the path maybe a major factor in explaining the differences between the observed and predicted path loss. However, our present modeling explains the 60dB signal enhancement above what one would expect under standard atmospheric conditions and seems to be a satisfactory first order approximation.

J. RICHTER (COMMENT)

In response to Professor Bach Andersen's question, horizontal inhomogeneity of ducting conditions along the path may certainly be one of the reasons for discrepancies between calculated and measured field strength values. Ducting parameters were measured only at one end of the propagation path and horizontal homogeneity was assumed along the path.

D. HÖHN

Are similar effects possible over land, under specific conditions, like melting snow, after rain, etc?

AUTHOR'S REPLY

In my opinion, it is unlikely to see similar effects over land. The surface would have to be relatively smooth over ranges of tens of kilometers and provide an unlimited moisture source.